N_2 and CO molecules as probes of zeolite acidity: an infrared spectroscopy and density functional investigation

Konstantin M. Neyman [a], Paul Strodel [a], Sergey Ph. Ruzankin [b], Norbert Schlensog [c], Helmut Knözinger [c] and Notker Rösch [a]

[a] *Lehrstuhl für Theoretische Chemie, Technische Universität München, D-85747 Garching, Germany*

[b] *Boreskov Institute of Catalysis, Russian Academy of Sciences, Prosp. Lavrentieva 5, 630090 Novosibirsk, Russia*

[c] *Institut für Physikalische Chemie, Universität München, Sophienstrasse 11, D-80333 Munich, Germany*

Received 19 August 1994; accepted 15 December 1994

The interaction of N_2 with Brønsted acid centers of H-ZSM-5 zeolite has been investigated employing Fourier transform infrared spectroscopy and cluster model calculations based on a gradient corrected density functional method. A comparison is made with CO, which is widely used as a probe for surface acidity. It is shown that the computational approach is capable of almost quantitatively reproducing a number of sensitive parameters of the H-bonded dinitrogen and carbonyl complexes, like adsorption energy, adsorption-induced changes of the vibrational frequencies and of their intensities. According to a constraint space orbital variation analysis, the carbonyl and dinitrogen complexes mainly differ by the somewhat stronger σ donation ability of CO as compared to N_2. It is concluded that dinitrogen may serve as a convenient probe for the acidity of zeolites.

Keywords: Brønsted acidity of zeolites; N_2 and CO probes; H-bonding; FTIR spectroscopy; adsorption-induced change of vibrational frequencies and intensities; density functional cluster models; gradient corrected exchange–correlation functionals

1. Introduction

The surface acidity of catalytic materials may be studied by infrared (IR) spectroscopy provided suitable probe molecules are available. Carbon monoxide has been demonstrated to be a convenient, sensitive and specific probe (ref. [1] and references therein). The isoelectronic N_2 probe, on the other hand, has rarely been employed up to now [2–5] in spite of the fact that the adsorption-induced IR activity of nonpolar diatomic molecules offers some advantage because no absorbance of gas phase molecules in the sample interferes with the relevant signal due to the adsorbed species.

The adsorption of a CO probe on an acidic bridging OH group in zeolites has been studied by model cluster calculations at the Hartree–Fock (HF) and electron correlation (MP2) levels of theory (e.g. refs. [6,7]). However, we are not aware of similar quantum chemical studies of complexes with the N_2 probe. To interpret the IR spectra of the species with adsorbed N_2 one often postulates an analogy between the carbonyl and dinitrogen adsorbates [3]. It is interesting to compare carbonyl and dinitrogen complexes theoretically and to identify those characteristic features of the electronic structure of CO and N_2 that are responsible for the differences in their bonding properties, in particular for their interaction with acidic hydroxyl groups.

The magnitude of the adsorption-induced red shift of the O–H frequency and of the blue shift of the intra-adsorbate C–O frequency in weakly bonded OH···CO complexes is crucial for quantifying the acid strength of OH groups: the larger the red shift $\Delta\omega_{O-H}$ and the blue intra-adsorbate frequency shift $\Delta\omega_{C-O}$, the greater the acid strength [1,8]. Results of small cluster models computed in the HF and MP2 approximations [6,7] tend to underestimate the observed red shift of the O–H frequency, but reasonably reproduce the blue C–O frequency shift [6]. Several reasons, like limitations of the cluster model, failure of the HF theory as well as the anharmonicity of the O–H mode have been suggested to explain this underestimation of the shift $\Delta\omega_{O-H}$ [6]. As the modeling of these frequency shifts is important for a thorough understanding of the probe–substrate interaction it seems appropriate to examine the performance of an alternative modern quantum chemical approach, density functional (DF) theory, in reproducing the characteristics of the adsorption complexes. The quantities of interest comprise both the observed trends and magnitudes of vibrational parameters, but also the adsorption energies and the structure of the dinitrogen and carbonyl complexes. This problem has another, more fundamental aspect: how accurate, in general, is a DF description of weak interactions of the van der Waals type? Recently, first attempts to answer this question [9,10] gave encouraging results when gradient corrections to the exchange–correlation potential were taken into account.

The present study is devoted to a comparison of N_2 and CO molecules as probes of Brønsted acidity of aluminosilicates. Fourier transform infrared (FTIR) spectra of H-ZSM-5 zeolites with negligibly small concentration of extra-framework cationic centers (Lewis acid sites) [11] and of the corresponding hydrogen bonded dinitrogen and carbonyl complexes were measured. The vibrational spectroscopy (frequencies and integral intensities), structural and bonding parameters were calculated using a gradient corrected version of the linear combination of the Gaussian-type orbitals density functional (LCGTO-DF) cluster method and a model cluster approach for the bridging –Si(OH)Al– group with and without CO and N_2 adsorbates. For the first time in combination with a DF method, the constrained space orbital variation (CSOV) analysis [12] is applied to quantify various contributions to the OH···CO and OH···N_2 bonds.

2. Experimental details

The H-ZSM-5 zeolite was from Degussa AG (Hanau, Germany) and had a n_{Si}/n_{Al} ratio of 28. For IT spectroscopy self-supporting wafers were pressed between mica platelets under a pressure of 15×10^6 Pa for 10 min. The resulting wafers had an areal density of 4–7 mg/cm^2. These specimens were pretreated in situ in the heating zone of the IR cell in flowing oxygen (50 cm^3/min) while increasing the temperature with a rate of 10 K/min from room temperature to 673 K, at which temperature the sample was held for 2 h. Prior to cooling to liquid N_2 temperature, the wafer was evacuated (ca. 10^{-3} Pa) at 673 K for 2 h.

Oxygen and nitrogen were from Linde AG and had purities of 99.995 and 99.999%, respectively. They were further purified and dried by passing them over Chrompack columns. $^{15}N_2$ was from CAMPRO Scientific. Its isotopic purity was greater than 99%.

The IR spectra were recorded at a spectral resolution of 1 cm^{-1} on a Brucker IFS 66 Fourier transform spectrometer. The in situ low-temperature transmission cell has been described previously [13].

3. Computational details

The "first principles" LCGTO-DF cluster method [14–16] was employed. Self-consistent calculations were performed using the standard local density approximation (LDA) to the exchange–correlation energy functional [17]. Once self-consistency is obtained, gradient corrections to the exchange [18] and to the correlation energy functional [19,20] are evaluated using the LDA density to improve the description of the energetics. This post-hoc procedure to account for non-local contributions to the exchange–correlation functional is quite economic and has been found to yield results of adequate accuracy [21].

The construction of the orbital basis started from basis sets of the types (12s9p) [22] for Si and Al, (9s5p) [23] for C, N, and O, and (6s) [23] for H. These basis sets were extended by two polarization exponents each, either of d-type (Si: 1.1206, 0.3202; Al: 1.0084, 0.2881; C: 1.9569, 0.5591; N: 1.9036, 0.5875; O: 1.0757, 0.3074) or of p-type (H:1.8708, 0.5345). The final sets have been contracted using generalized contractions [24] based on LDA atomic eigenvectors as follows: Si, Al (12s9p2d) → [6s4p2d]; C, N, O (9s5p2d) → [5s4p2d]; H (6s2p) → [3s2p]. The two auxiliary basis sets used in the LCGTO-DF method to represent the electron charge density and the exchange–correlation potential were constructed from the orbital exponents in a standard fashion [15,25].

The basic cluster models employed in the present study are displayed in fig. 1. Brønsted acid sites (bridging OH groups) were modeled by the cluster $H_3Si(OH)AlH_3$ of C_s symmetry in two different conformations of the AlH_3 fragment (clusters A and B). The H–T bond-length (T = Si, Al) was taken to be

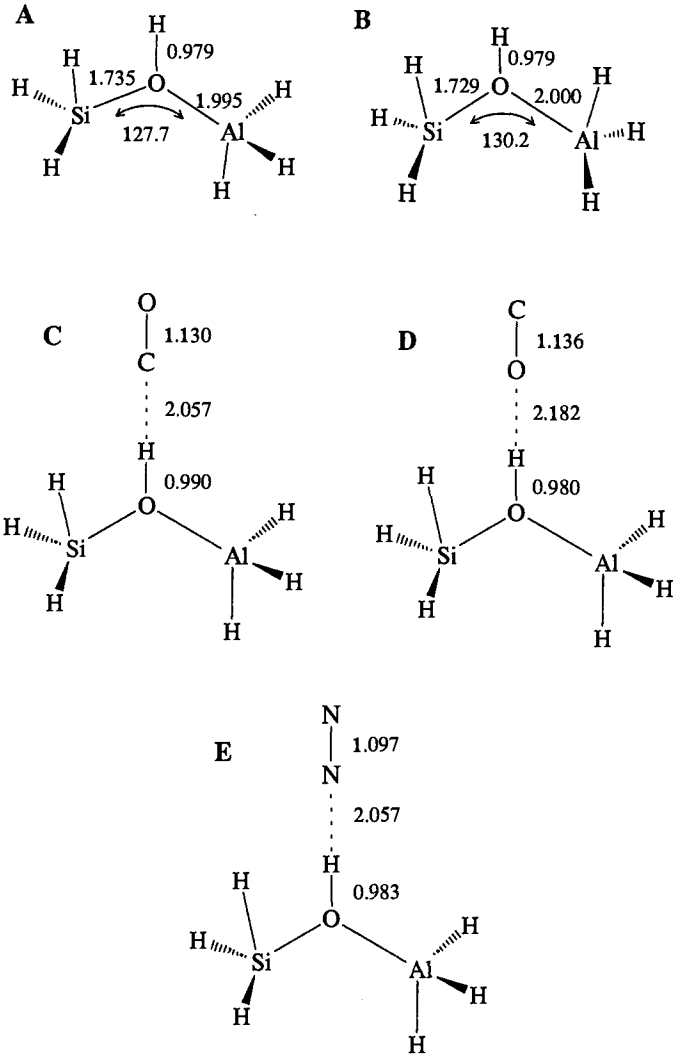

Fig. 1. Cluster models and calculated structural parameters (bond lengths in angstrøm, angles in degrees) of the Brønsted acid site in aluminosilicates (bridging OH group) $H_3Si(OH)AlH_3$ (A, B), and of adsorption complexes $H_3Si(OH)AlH_3$–CO (C), $H_3Si(OH)AlH_3$–OC (D), and $H_3Si(OH)AlH_3-N_2$ (E). Only values of the structural parameters optimized for a given cluster model are shown (see section 3).

equal to that computed for the tetrahedral TH_4 clusters, H–Si = 1.497 Å and H–Al = 1.655 Å. The H_3TO moieties were assumed to have local symmetry C_{3v} with HTH angles as in the tetrahedron (109.47°). The angles TOH were kept equal in the course of the geometry optimization. Other structural parameters of the clusters (see fig. 1) have been optimized without further constraints. The total energy difference for the models A and B is only 0.015 eV (1 eV/molecule = 96.48 kJ/mol) slightly favoring conformation A. Furthermore, such a change of the confor-

mation results in a negligible difference of the properties of the OH group – ω_{O-H} = 3459 cm^{-1} (model A) versus 3463 cm^{-1} (model B). For complexes B–E with adsorbed CO and N_2 and the O–H bond length has been reoptimized. The conformation of clusters A, C, and D corresponds to a global energy minimum if fully optimized at the HF or MP2/DZP level of theory [7].

A cyclic optimization strategy of all varied degrees of freedom (two complete cycles sufficed) was used to search for the equilibrium geometry of the substrate cluster and of adsorption complexes where the adsorbed molecule was assumed to be oriented upright along the z axis (fig. 1). The binding energies were corrected for the basis set superposition error (BSSE) with the help of the counterpoise technique [26], but no zero-point correction was applied. Harmonic (ω_e) and anharmonic (energies of the $0 \rightarrow 1$ transition between the vibrational levels, ω) vibrational frequencies were computed by fitting a polynomial to seven points of the potential curve located near the minimum. The normal modes of the substrate and adsorption complexes have been approximated by the computed O–H, C–O, or N–N internal modes, respectively.

Absolute IR intensities (integrated absorption coefficients) have been calculated in the double-harmonic approach [27] according to which an IR intensity is proportional to the square of the dynamic dipole moment of the normal mode, i.e. to the square of the partial derivative of the total dipole moment μ with respect to the corresponding nuclear displacement. Dynamic dipole moments $\partial\mu/\partial r$ were calculated from a parabolic approximation defined by three points near the equilibrium.

The nature of the OH···CO and OH···N_2 chemical bonds has been analyzed with the help of a CSOV procedure [12] which was used up to now exclusively within the HF approach. Here we present results of the first CSOV application to DF results. The CSOV analysis attempts to separate and to quantify various energy contributions to the bonding of two fragments. The starting point of this procedure is a total energy calculation for a charge density constructed by superimposing charge densities obtained from separate calculations of the adsorbate and the substrate fragments at their equilibrium geometry. The Kohn–Sham orbitals of one fragment are orthogonalized to those of another fragment. The energy difference relative to the sum of the total energies of the isolated fragments is taken to represent the compound effect of *Pauli repulsion* between the two fragments and of the *electrostatic interaction* in the frozen orbital approximation. In step 2 of the CSOV analysis, the *polarization of the adsorbate* is investigated by allowing only an orbital variation within the space of the occupied and vacant orbitals of the adsorbate in the presence of a frozen substrate. The contribution to the binding energy of the *adsorbate-to-substrate charge transfer* is then characterized by including the unoccupied substrate orbitals in the variation space (step 3). The occupied orbitals of the adsorbate resulting in step 3 are kept frozen during the subsequent steps 4 and 5. The latter steps aim at the evaluation of bonding contributions due to the *substrate polarization* and to the *substrate-to-adsorbate charge transfer*, respec-

tively. They are performed in a way analogous to steps 2 and 3. In steps 3 and 5, the charge transfer contributions of orbitals belonging to different irreducible representations may be separated. Details of the CSOV implementation in the LCGTO-DF code and other methodological aspects of DF computations on adsorbate–substrate interactions will be discussed elsewhere [28].

4. Results and discussion

4.1. EXPERIMENTAL RESULTS

The background spectrum of the H-ZSM-5 sample in the hydroxyl stretching region (3850–3500 cm^{-1}) is shown in fig. 2A. The spectrum was recorded at 83 K after standard pretreatment at 673 K and evacuation. The principal band is located at 3615 cm^{-1} with a band half-width of 34 cm^{-1}. This band is assigned as the O–H stretching mode of the acidic bridging framework OH groups of the type Si(OH)Al as frequently reported in the literature [29–31]. In addition, a relatively weak band at 3745 cm^{-1}, which is asymmetric towards lower wavenumbers, is observed which is attributed to isolated silanol groups located on the external surface of zeolites and silicates [29,32] and to terminal OH groups of chains of H-bonded silanol groups (asymmetry) [32].

When $^{14}N_2$ or $^{15}N_2$ was adsorbed (fig. 2A), the band of the acidic OH groups at 3615 cm^{-1} was significantly reduced in intensity while the band of silanol groups

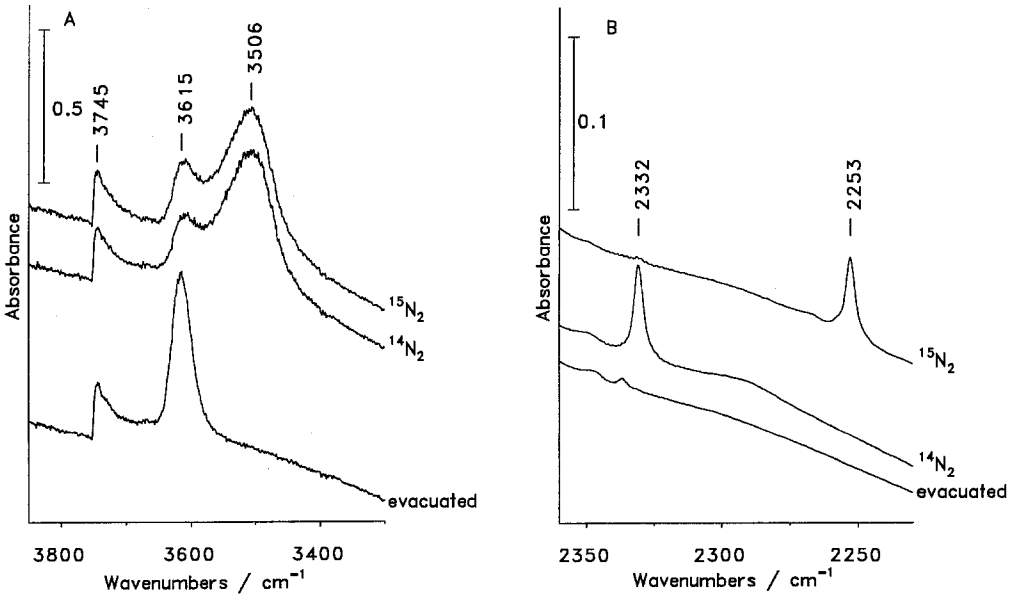

Fig. 2. FTIR spectra of H-ZSM-5 and of the adsorption complexes with N_2. (A) O–H stretching region; (B) N–N stretching region. 35 hPa dinitrogen were adsorbed at 173 K.

remained essentially unperturbed (under the conditions used). Simultaneously, a new broad band developed at 3506 cm^{-1} with a band half-width of almost 100 cm^{-1}. The frequency shift of 109 cm^{-1} relative to the position of the unperturbed O–H stretching mode, the increase in band width and the enhanced integral intensity of the band are characteristic of hydrogen-bonding interactions. The experimental O–H frequency shift is also included in table 1.

The corresponding vibrational spectra in the N–N stretching region are reproduced in fig. 2B. Adsorption of $^{14}N_2$ gives rise to a clearly detectable band at 2332 cm^{-1}, this band position being shifted to higher wavenumbers by 2 cm^{-1} relative to the reported Raman band position at 2330 cm^{-1} [33]. The corresponding band for adsorbed $^{15}N_2$ is observed at 2253 cm^{-1}, this position being shifted to lower wavenumbers by the theoretically predicted isotope shift of 79 cm^{-1}. The bands observed in this frequency range are therefore to be attributed without doubt to the N–N stretching mode of adsorbed N_2 molecules. This clearly indicates a symmetry reduction due to the adsorption interaction. Similar band positions for N_2 adsorbed on H-ZSM-5 have been reported by Wakabayashi et al. [5].

Carbon monoxide adsorption data have been reported by several groups in the recent past [11,29–31]. The CO molecule is supposed to undergo a 1 : 1 H-bonding interaction of the type OH···CO with the acidic OH groups. The observed frequency shift of 312 cm^{-1} for the O–H stretching mode is consistent with this type of adsorption bonding and with the expected greater heat of adsorption as compared to N_2. The experimental frequency shift is also included in table 1 for comparison. On adsorption the carbonyl stretching frequency was observed at 2175 cm^{-1} [11], i.e. shifted to higher wavenumbers by 32 cm^{-1} (see table 1) relative to the gas phase frequency, this again being qualitatively consistent with the proposed H-bonding interaction.

4.2. QUANTUM CHEMICAL RESULTS

The various calculated results are summarized in table 1. It should be noted that the size of the employed cluster models (fig. 1) is too small to reproduce differences in the acidity and in the vibrational parameters of the bridging OH group for various types of zeolites. Fortunately, these properties do not strongly depend on the structure of a zeolite, rather the observed differences are generally comparable to the deviations between measured and calculated results. For example, the vibrational frequency of bridging OH groups in H-mordenite, H-Y and H-ZSM-5 zeolites is measured to lie in the narrow interval 3616–3619 cm^{-1} [4,5]. A similar observation holds for the adsorption-induced frequency shifts. If one incorporates next-nearest neighbors of the OH group into the cluster only minor changes in the calculated acidity and vibrational properties result [34]. Therefore, the cluster model $H_3Si(OH)AlH_3$ seems adequate for the description of the bridging OH group in aluminosilicates in general. This model has been considered many times in the past (ref. [6] and references therein). We decided to carry out only a partial geom-

Table 1
Calculated and experimental parameters for the Brønsted site –Si(OH)Al–, for free CO and N_2 molecules as well as for the H-bonded adsorption complexes. d_{OH-ads}, distance between the H atom and the closest atom of the adsorbate; $\Delta\omega_{O-H}$, O–H frequency shift; $\Delta\omega_{e\,O-H}$, harmonic O–H frequency shift; I_{O-H}, absolute IR intensity of the O–H mode; $\partial\mu/\partial r_{O-H}$, dynamic dipole moment of the O–H mode; r_e, equilibrium C–O or N–N bond length; $\Delta\omega_{ads}$, frequency shift of the intra-adsorbate mode; I_{ads}, absolute IR intensity of the intra-adsorbate mode; $\partial\mu/\partial r_{ads}$, dynamic dipole moment of the intra-adsorbate mode; D_e, adsorption energy; D_e^{BSSE}, adsorption energy corrected for the basis set superposition error

System	d_{OH-ads} (Å)	$\Delta\omega_{O-H}$ (cm^{-1})	$\Delta\omega_{e\,O-H}$ (cm^{-1})	I_{O-H} (km/mol)	$\partial\mu/\partial r_{O-H}$ (a.u.)	r_e (Å)	$\Delta\omega_{ads}$ (cm^{-1})	I_{ads} (km/mol)	$\partial\mu/\partial r_{ads}$ (a.u.)	D_e (eV)	D_e^{BSSE} (eV)
$H_3Si(OH)AlH_3$											
DFT	–	3459[a]	3625[a]	141	0.37	–	–	–	–	–	–
exper.	–	3615[a]				–	–	–	–	–	–
$H_3Si(OH)AlH_3$–CO											
DFT	2.06	−293	−230	953	0.96	1.130	43	58	−0.64	0.23	0.19
exper.		−312					32				
CO											
DFT	–	–	–	–	–	1.134	2120[a]	59	−0.64	–	–
exper. [33]	–	–	–	–	–	1.128	2143[a]	60.5	−0.65	–	–
$H_3Si(OH)AlH_3$–N_2											
DFT	2.06	−109	−107	683	0.82	1.097	−4	3	0.16	0.16	0.11
exper.		−109					2				
N_2											
DFT	–	–	–	–	–	1.099	2364[a]	0	0.00	–	–
exper. [33]	–	–	–	–	–	1.098	2330[a]	0	0.00	–	–

[a] Reference values for the frequency shift.

etry optimization keeping the TH_3 fragments fixed in order to take into account the boundary conditions imposed by the surrounding lattice which is absent in the cluster models. The two cluster conformations (figs. 1A and 1B) do not differ significantly, neither in the geometry nor in O–H frequency ($\Delta\omega_{O-H} = 4$ cm^{-1}).

The results of the gradient corrected DF description of the adsorbate (table 1) exhibit very good accuracy for the whole set of computed parameters. The correct sign and value of the CO electric dipole moment and its derivative with respect to the interatomic bond length provide a most sensitive test for the accuracy of the computational method. The results also provide evidence for the expected level of reliability of calculated vibrational intensities discussed below. For the model $H_3Si(OH)AlH_3$ the O–H frequency is notably underestimated compared to the experimental value. As will be shown elsewhere [28], this deficiency is inherent to all calculations using various types of both local and gradient corrected exchange–correlation density functionals. Furthermore, the cluster size also seems to contribute to the underestimation of the O–H frequency. Similar reasons are probably responsible for an overestimation of the extinction coefficient of the unperturbed O–H groups calculated in the double-harmonic approach [27] (table 1) compared to the value of 85 km/mol [35] measured recently for a HY zeolite (Si/Al = 2.7). One should mention, however, that the extinction coefficient depends markedly on the degree of the exchange, on the calcination temperature and on other experimental conditions. So, the experimental values of the extinction coefficient reported so far cover a very wide range from 31 to 199 km/mol (ref. [35] and references therein).

The adsorption-induced frequency shifts for the carbonyl and the dinitrogen complexes $\Delta\omega_{O-H}$ and $\Delta\omega_{C-O}$ or $\Delta\omega_{N-N}$ are in good agreement with the measured values (see table 1). It should be stressed that these are the observables employed as a measure for the acidity of surface OH groups. An almost vanishing shift of the N–N frequency for the dinitrogen complex compared to free N_2 is measured and calculated. The larger C–O frequency shift reflects a stronger OH$\cdots$CO bonding relative to OH$\cdots N_2$, in agreement with a higher proton affinity of CO compared to that of N_2 [36]. The adsorption is accompanied by a red shift of the O–H band which is again larger for the CO adsorbate. It is worth mentioning that the agreement with the measured shift $\Delta\omega_{O-H}$ for carbonyl is much better when the anharmonicity of the O–H mode is taken into account as it displays a significant change upon adsorption (by 63 cm^{-1}). This finding may partly explain why the CO-induced shift $\Delta\omega_{O-H}$ for the same cluster model $H_3Si(OH)AlH_3$–CO is substantially lower in an HF study where only *harmonic* frequencies have been considered [6,7]. Inspection of table 1 reveals that the change in the anharmonicity of the O–H mode due to the formation of the dinitrogen complex is much smaller as a consequence of the weaker interaction with N_2.

Another important aspect of the adsorption of the probe molecules is the change of the integral intensity of the vibrational bands compared to those of the isolated adsorbate and substrate fragments. The most extreme case is the N_2 molecule for

which the IR forbidden N–N vibration becomes allowed by the interaction with the substrate and the absorbance increases from zero to a measurable value. According to the computed data the absolute IR N–N intensity of the adsorbed N_2 is more than an order of magnitude smaller than that of the strongly absorbing C–O mode. As has been shown in section 4.1, this is sufficient to measure the adsorption-induced N–N mode in IR. On the other hand, the hydrogen bonding interaction has essentially no effect on the intensity of the C–O mode. For both CO and N_2 adsorption, DF calculations predict a very significant increase of the IR intensity of shifted O–H bands compared to the intensity of the $H_3Si(OH)AlH_3$ cluster. Qualitatively, the experimental spectra in fig. 2 and those for CO adsorption are in general agreement with the DF results. As can be estimated from the spectra of fig. 2A, the ratio of the integrated intensities of the perturbed by N_2 adsorption and of the unperturbed O–H stretching band is approximately 3, whereas the calculated value (see table 1) is about 4.8. For interactions with CO the calculated ratio of the O–H IR intensities, 6.8 (table 1), is close to the experimental ratio of approximately 8.

According to the results of the CSOV analysis (table 2), the main contribution to the hydrogen bonding comes, as expected, from a charge transfer to the substrate. The difference in the bond strength of the adsorbate-to-substrate bond between CO and N_2 is mostly due to the fact that the latter species is a weaker σ donor compared to carbon monoxide. The stronger σ bonding of CO is consistent with a stronger localization of the CO 5σ orbital in the region of the hydrogen bond. One may see from table 2 that all other computed contributions to adsorption bonds are smaller and differ only slightly between the two adsorbates. These small contributions should be considered only with great care because they are comparable in magnitude to the basis set superposition error for CO and N_2, 0.04–0.05 eV (table 1). In summary, the CSOV analysis reveals that the adsorption bonds are formed mainly due to σ charge transfer from the adsorbate to the substrate and, less importantly, to the polarization of the adsorbate and of the substrate.

Table 2
CSOV analysis of various contributions to the calculated interaction energy, ΔE (eV), of CO and N_2 molecules with the Brønsted acid site $H_3Si(OH)AlH_3$

Cluster model	$H_3Si(OH)AlH_3-N_2$	$H_3Si(OH)AlH_3-CO$
1. Pauli repulsion + "frozen orbital" attraction	−0.018	−0.010
2. polarization of the adsorbate	0.041	0.050
3. charge transfer adsorbate → substrate	0.121	0.169
4. polarization of the substrate	0.013	0.026
5. charge transfer substrate → adsorbate	0.000	0.000
total CSOV	0.157	0.234
SCF	0.157	0.234

π complexes of both dinitrogen and carbon monoxide (side-on configuration) were found to be unbound at the present level of cluster calculations. Consequently, for dinitrogen the end-on configuration (OH···N–N) as shown in fig. 1E is the most likely adsorption structure. In the case of carbon monoxide the oxygen-down adsorption on the bridging OH group gives a computed value of the binding energy of only 0.06 eV (corrected for BSSE), of the OH···OC bond length of 2.182 Å and of the frequency shifts $\Delta\omega_{O-H} = -14$ cm^{-1} and $\Delta\omega_{C-O} = -22$ cm^{-1}. The computed binding energy for this bonding geometry turns out to be significantly lower than that obtained for a carbon-down geometry, namely 0.19 eV (vide supra). Moreover, the magnitudes of the calculated frequency shifts deviate from the experimental data and for the carbonyl frequency even the sign of the shift is opposite. It must therefore be concluded that CO is most probably bonded to an OH group via its C atom. The same conclusion concerning possible CO orientations has been drawn based on HF and electron correlation calculations for the interaction with bridging OH groups [6,7] and with silanol hydroxyl groups [6,37].

It is interesting to note that the calculated interaction energy for the OH···N–N dinitrogen complex (0.11 eV) is very close to the value of 0.12 eV determined experimentally from temperature dependence of IR intensities for N_2 adsorption on H-mordenite [4]. In contrast, the spectroscopically determined binding energy for CO on bridging OH groups in HY zeolites was reported to be only 0.12 eV [38], while the computed value as found in the present study is 0.19 eV. These coincidences and discrepancies between calculated and spectroscopically determined binding energies should certainly not be overestimated. The experimental values may not be very accurate, since the measurement of the temperature of the wafer in the IR beam is extremely critical, thus introducing a significant error in the derived thermodynamic data. On the other hand, accuracy limitations of the computational approach and of small cluster models employed may also affect calculated binding energies to a certain extent.

5. Conclusions

A combined LCGTO-DF model cluster and FTIR spectroscopic study of adsorption complexes of N_2 and CO molecules with Brønsted acid sites in zeolites has been performed. The main results may be summarized as follows:

(1) Both N_2 and CO interact with the acidic OH group in an end-on configuration. The preferred bonding of CO to the OH group is via the C atom.

(2) The dinitrogen molecule has been shown to be a specific and convenient probe of Brønsted acidity of aluminosilicates. The adsorption-induced shift of the O–H (to the red) and N–N frequencies (slightly to the blue) as well as an increase of the integral intensity of the O–H stretching mode are qualitatively similar to those observed for CO adsorption. However, the perturbation of the acidic OH group caused by CO molecules is significantly stronger. A distinct advantage of the homo-

nuclear N_2 probe is that only adsorbed species are IR active and that the spectra do not need to be corrected for the absorbance of gas phase molecules.

(3) It has been demonstrated that the LCGTO-DF method employing a gradient corrected exchange–correlation energy functional is adequate to describe very sensitive parameters of weakly bound adsorption complexes with Brønsted acid sites, even in the approximation of small cluster models. At variance with the HF and MP2 approaches (where no anharmonicity of the O–H is taken into account) the DF method is capable of accurately representing the frequency shifts induced by the adsorption of CO and N_2, not only for the intra-adsorbate, but also for the O–H modes. The calculated DF data are also in good agreement with the observed trends of other characteristics of the dinitrogen and carbonyl complexes: the differences in the adsorption energy as well as in the adsorption-induced changes of the integral extinction coefficient of the O–H band. The accuracy of the DF method established here is of extreme importance for applications to H-bonded systems and other van der Waals complexes in general.

(4) To provide a physically and chemically significant analysis of the bonding mechanism in OH···CO and OH···N_2 complexes and to identify the reasons for the somewhat different behavior of N_2 and CO as ligands, the LCGTO-DF code has been augmented for performing a CSOV procedure which has been applied here for the first time within the DF framework. According to the CSOV results and not unexpectedly, the main contribution to the hydrogen bonding stems from the σ charge transfer to the substrate. The difference in the bond strength of CO and N_2 is mostly due to the fact that dinitrogen is a weaker σ donor than carbon monoxide.

Acknowledgement

The authors are grateful to Dr. I.N. Senchenya for fruitful discussions and for communicating results prior to publication. Financial support by the Bayerischer Forschungsverbund Katalyse, by the Deutsche Forschungsgemeinschaft, by the Fonds der Chemischen Industrie and by the Volkswagen-Stiftung (Project I/68 691) is gratefully acknowledged.

References

[1] H. Knözinger, in: *Elementary Reaction Steps in Heterogeneous Catalysis*, eds. R.W. Joyner and R.A. van Santen (Plenum Press, New York, 1993) p. 267.
[2] S.A. Zubkov, V.Y. Borovkov, S.G. Gagarin and V.B. Kazansky, Chem. Phys. Lett. 107 (1984) 337.
[3] S.M. Zverev, K.S. Smirnov and A.A. Tsyganenko, Kinet. Katal. 29 (1988) 1439.
[4] F. Wakabayashi, J. Kondo, A. Wada, K. Domen and C. Hirose, J. Phys. Chem. 97 (1993) 10761.

[5] F. Wakabayashi, J. Kondo, K. Domen and C. Hirose, Catal. Lett. 21 (1993) 257.
[6] S. Bates and J. Dwyer, J. Phys. Chem. 97 (1993) 5897.
[7] I.N. Senchenya, private communication.
[8] H. Knözinger, in: *Adsorption on Ordered Surfaces of Ionic Solids and Thin Films*, Springer Series in Surface Sciences, Vol. 33, eds. H.-J. Freund and E. Umbach (Springer, Berlin, 1993) p. 257.
[9] F. Sim, A. St-Amant, I. Papai and D.R. Salahub, J. Am. Chem. Soc. 114 (1992) 4391.
[10] T. Oie, I.A. Topol and S.K. Burt, J. Phys. Chem. 98 (1994) 1121.
[11] I. Mirsojew, S. Ernst, J. Weitkamp and H. Knözinger, Catal. Lett. 24 (1994) 235.
[12] P.S. Bagus, K. Hermann and C.W. Bauschlicher Jr., J. Chem. Phys. 80 (1984) 4378.
[13] G. Künzmann, Doctoral Thesis, University of Munich, Germany (1987).
[14] N. Rösch, P. Knappe, P. Sandl, A. Görling and B.I. Dunlap, in: *The Challenge of d and f Electrons. Theory and Computation,* ACS Symposium Series No. 394, eds. D.R. Salahub and M.C. Zerner (Am. Chem. Soc., Washington, 1989) p. 180.
[15] B.I. Dunlap and N. Rösch, Advan. Quantum Chem. 21 (1990) 317.
[16] N. Rösch, in: *Cluster Models for Surface and Bulk Phenomena*, NATO ASI Series B, eds. G. Pacchioni, P.S. Bagus and F. Parmigiani (Plenum Press, New York, 1992) p. 251.
[17] S.H. Vosko, L. Wilk and M. Nusair, Can. J. Phys. 58 (1980) 1200.
[18] A.D. Becke, Phys. Rev. A 38 (1988) 3098.
[19] C. Lee, W. Yang and R.G. Parr, Phys. Rev. B 37 (1988) 785.
[20] B. Miehlich, A. Savin, H. Stoll and H. Preuss, Chem. Phys. Lett. 157 (1989) 200.
[21] L. Fan and T. Ziegler, J. Chem. Phys. 94 (1991) 6057.
[22] A. Veillard, Theoret. Chim. Acta. 12 (1968) 168.
[23] F.B. van Duijneveldt, IBM Res. Report No. RJ 945 (1971).
[24] R.C. Raffenetti, J. Chem. Phys. 58 (1973) 4452.
[25] H. Jörg, N. Rösch, J.R. Sabin and B.I. Dunlap, Chem. Phys. Lett. 114 (1985) 529.
[26] S.F. Boys and F. Bernardi, Mol. Phys. 19 (1970) 553.
[27] R.D. Amos, Advan. Chem. Phys. 67 (1987) 99.
[28] K.M. Neyman, S.P. Ruzankin and N. Rösch, to be published.
[29] L.M. Kustov, V.B. Kazansky, S. Beran, L. Kubelková and P. Jiru, J. Phys. Chem. 91 (1987) 5247.
[30] L. Kubelková, S. Beran and J.A. Lercher, Zeolites 9 (1989) 539.
[31] A. Zecchina, S. Bordiga, G. Spoto, D. Scarano, G. Petrini, G. Leofanti, M. Padovan and C. Otero Areán, J. Chem. Soc. Faraday Trans. 88 (1992) 2959.
[32] A. Zecchina, S. Bordiga, G. Spoto, L. Marchese, G. Petrini, G. Leofanti and M. Padovan, J. Phys. Chem. 96 (1992) 4991.
[33] K.P. Huber and G. Herzberg, *Constants of Diatomic Molecules,* Molecular Spectra and Molecular Structure, Vol. 4 (Van Nostrand Reinhold, New York, 1979).
[34] A.G. Pelmenshchikov, E.A. Paukshtis, V.G. Stepanov, V.I. Pavlov, E.N. Yurchenko, K.G. Ione and G.M. Zhidomirov, J. Phys. Chem. 93 (1989) 6725.
[35] M.A. Makarova, A.F. Ojo, K. Karim, M. Hunger and J. Dwyer, J. Phys. Chem. 98 (1994) 3619.
[36] S.G. Lias, J.F. Liebman and R.D. Levin, J. Phys. Chem. Ref. Data 13 (1984) 695.
[37] P. Ugliengo, V.R. Saunders and E. Garrone, J. Phys. Chem. 93 (1989) 5210.
[38] N. Echoufi and P. Gélin, J. Chem. Soc. Faraday Trans. 88 (1992) 1067.